




Article

TDP-43 and Alzheimer's Disease Pathology in the Brain of a Harbor Porpoise Exposed to the Cyanobacterial Toxin BMAA

Susanna P. Garamszegi ^{1,†}, Daniel J. Brzostowicki ^{1,†}, Thomas M. Coyne ², Regina T. Vontell ¹
and David A. Davis ^{1,*}

¹ Department of Neurology, Miller School of Medicine, University of Miami, Miami, FL 33136, USA

² Department of Pathology, Immunology and Laboratory Medicine, University of Florida, Gainesville, FL 32610, USA

* Correspondence: d.davis12@med.miami.edu

† These authors contributed equally to this work.

Abstract: Cetaceans are well-regarded as sentinels for toxin exposure. Emerging studies suggest that cetaceans can also develop neuropathological changes associated with neurodegenerative disease. The occurrence of neuropathology makes cetaceans an ideal species for examining the impact of marine toxins on the brain across the lifespan. Here, we describe TAR DNA-binding protein 43 (TDP-43) proteinopathy and Alzheimer's disease (AD) neuropathological changes in a beached harbor porpoise (*Phocoena phocoena*) that was exposed to a toxin produced by cyanobacteria called β -N-methylamino-L-alanine (BMAA). We found pathogenic TDP-43 cytoplasmic inclusions in neurons throughout the cerebral cortex, midbrain and brainstem. P62/sequestosome-1, responsible for the autophagy of misfolded proteins, was observed in the amygdala, hippocampus and frontal cortex. Genes implicated in AD and TDP-43 neuropathology such as *APP* and *TARDBP* were expressed in the brain. AD neuropathological changes such as amyloid- β plaques, neurofibrillary tangles, granulovacuolar degeneration and Hirano bodies were present in the hippocampus. These findings further support the development of progressive neurodegenerative disease in cetaceans and a potential causative link to cyanobacterial toxins. Climate change, nutrient pollution and industrial waste are increasing the frequency of harmful cyanobacterial blooms. Cyanotoxins like BMAA that are associated with neurodegenerative disease pose an increasing public health risk.



Citation: Garamszegi, S.P.; Brzostowicki, D.J.; Coyne, T.M.; Vontell, R.T.; Davis, D.A. TDP-43 and Alzheimer's Disease Pathology in the Brain of a Harbor Porpoise Exposed to the Cyanobacterial Toxin BMAA. *Toxins* **2024**, *16*, 42. <https://doi.org/10.3390/toxins16010042>

Received: 29 November 2023

Revised: 30 December 2023

Accepted: 10 January 2024

Published: 12 January 2024



Copyright: © 2024 by the authors. Licensee MDPI, Basel, Switzerland. This article is an open access article distributed under the terms and conditions of the Creative Commons Attribution (CC BY) license (<https://creativecommons.org/licenses/by/4.0/>).

Keywords: blue green algae bloom; cetacean stranding; Guam ALS/PDC; marine neurotoxin; marine food web; toothed whales

Key Contribution: TDP-43 proteinopathy and co-occurring Alzheimer's disease neuropathological changes were observed in the brain of a beach harbor porpoise that was exposed to the cyanotoxin BMAA.

1. Introduction

Cetaceans are considered one of the most intelligent species on earth with self-awareness, long-term memory and social recognition that can last for at least two decades [1]. They are long-lived mammals, with some species having an encephalization quotient that is far closer to humans than non-human primates and the great apes [2]. The complexity of their neuroanatomy, neurocircuitry, acoustic communication, sleep and social behavior has been a focus of research for many decades [3–5]. Recently, emerging evidence suggests that several cetacean species can also develop age-related neurodegenerative pathological changes reminiscent of those observed in Alzheimer's disease (AD) [6–11]. Cetaceans are also a well-regarded sentinel species for toxin exposures forewarning of the accumulation of toxic compounds in the marine environment [12–14]. Since cetaceans can develop AD-like neuropathological changes and are exposed to marine toxins throughout their

life span, they are an ideal model species to assess the long-term effects of neurotoxins on brain health.

β -N-methylamino-L-alanine (BMAA) is a non-canonical amino acid made by 95% of cyanobacteria genera [15,16]. Chronic dietary exposure to BMAA is associated with neurodegenerative disease in humans [17]. In the western Pacific, Guamanians with diets high in BMAA developed a complex neurodegenerative disease call *Lytico-bodig* or amyotrophic lateral sclerosis/parkinsonism-dementia complex (ALS/PDC), which consists of motor neuron degeneration and dementia [18–20]. The neuropathological changes in ALS/PDC include abundant cortical neurofibrillary tangles (NFTs), sparse-to-moderate amyloid- β ($A\beta$) plaques and TAR DNA-binding protein 43 (TDP-43) cytoplasmic inclusions (CI) [21,22]. These autopsy findings were further supported by non-human primate models that were fed high doses of BMAA and developed TDP-43 CI, NFTs and $A\beta$ deposits in their brain and spinal cord [23–25]. Outside of Guam, the BMAA toxin has been detected throughout the marine food web, including the brain and muscle tissues of apex predators [26–28]. BMAA has also been detected in autopsied brain samples and CSF of individuals with AD and ALS [29–31]. Thus, the presence of BMAA throughout the marine food web is a concern for apex predators and humans at risk of developing dementia and motor neuron disease. Because the detection of BMAA in human tissue can vary due to a number of factors, examining marine mammals that have a lifetime risk of cyanotoxin exposure may provide more consistent measurements and allow for novel insights into BMAA's mechanism of neurotoxicity [20,29,30,32,33].

We have previously reported that the BMAA toxin can bioaccumulate in the cerebral cortex of two dolphin species: *Tursiops truncatus* and *Delphinus delphis* [7]. The same dolphins displayed neuropathological changes reminiscent of AD and the severity of these neuropathological changes increased with BMAA exposure [6]. These studies suggest BMAA may have a role in the development of neurodegenerative phenotype in cetaceans. Here, we present a neurotoxicological analysis of a postmortem brain procured from a harbor porpoise (*Phocoena phocoena*) found beached in Cape Cod Bay, MA, USA. BMAA testing, qPCR analysis for genes implicated in dementia and motor neuron diseases and neuropathological evaluation were performed on corresponding brain regions implicated in AD and TDP-43 proteinopathies.

2. Results

2.1. Case History

In March 2012, a live female nonpregnant subadult harbor porpoise was reported stranded alone at Chapin Beach in Dennis, MA, USA (condition code 1) (LAT: 41.72697; LONG: -70.23891). The harbor porpoise was found in critical condition displaying signs of emaciation and scavenger trauma to the left eye caused by sea gulls. No human interactions were observed based on physical assessment. The harbor porpoise (ID: IFAW 12-206 Pp) was determined to be in poor health and was euthanized, followed by a necropsy where the weight (19 kg) and length were measured (1.1 m). The brain was removed, preserved and provided to the University of Miami Brain Endowment Bank (UMBEB) for gross, neuropathological and toxicological analysis.

2.2. Cyanobacterial Toxin BMAA Exposure

We detected BMAA in two adjacent cortical gyri of the parietal cortex (Pc) of IFAW 12-206 Pp: the auditory cortex or A1 (Pc^{A1}) ($93.6 \pm 9.1 \mu\text{g/g}$) and the visual cortex of V1 (Pc^{V1}) ($93.1 \pm 7.5 \mu\text{g/g}$). BMAA tissue concentrations did not differ between the two cortical gyri (Table 1). We also detected BMAA structural isomers: 2,4-diaminobutyric acid (2,4-DAB) and N-(2-aminoethyl)glycine (AEG). However, AEG was not detected in Pc^{V1} ($p = 0.001$, t -test) (Table 1). BMAA was 5.7 times more concentrated than AEG and 2.8 times less concentrated than 2,4-DAB. In addition, we observed a positive correlation between 2,4-DAB and BMAA brain tissue concentrations ($r = 0.7964$; $p = 0.01$, Pearson r).

No correlation with BMAA and AEG concentration was observed ($r = -0.2278$; $p = 0.4692$, Pearson r).

Table 1. BMAA and BMAA structural isomer detection in the brain of a beached harbor porpoise.

Brain Regions	BMAA ($\mu\text{g/g}$)	AEG ($\mu\text{g/g}$)	2,4-DAB ($\mu\text{g/g}$)
Pc ^{A1} ($n = 4$)	93.6 \pm 9.1 ^{ns}	36.5 \pm 7.7 ^{$p = 0.001$}	282.6 \pm 21.2 ^{ns}
Pc ^{V1} ($n = 5$)	93.1 \pm 7.5	ND	245.0 \pm 15.4
Mean + S.E.	93.3 \pm 5.4	16.2 \pm 7.2	261.7 \pm 13.6

A1: auditory cortex; ND: not detected; ns: no statistical significance; Pc: parietal cortex; V1: visual cortex.

2.3. Expression of Genes Implicated in Alzheimer's Disease and TDP-43 Proteinopathy

All dementia-related genes were expressed in each brain region analyzed from IFAW 12–206 Pp (Table 2). Six of the seven genes evaluated were expressed at higher levels in the cerebral cortex (Ctx) when compared to the cerebellum (CE), a region mostly unaffected in AD, ALS and frontal temporal dementia (FTD). One gene, presenilin-2 (*PSEN2*), was decreased in both Ctx regions. Gene expression patterns for Pc^{V1} and frontal cortex (Fc) were positively correlated ($r = 0.844$; $p = 0.017$, Pearson r) and mirrored the region-specific expression of genes in the Pc and prefrontal cortex (PreFc) of humans. The A β precursor protein (APP) (2.7-fold; $p < 0.0001$, ANOVA) and microtubule-associated protein tau (*MAPT*) (2.4-fold; $p = 0.0134$, ANOVA) were the most highly expressed genes in the Ctx. *TARBDP*, the gene that encodes for TDP-43 protein, was also expressed up to ~2.0-fold ($p = 0.0551$, ANOVA) more in the Ctx. These data suggest that the harbor porpoise displayed similar brain region-specific gene expression patterns as in humans.

Table 2. Comparative brain region specific gene expression of dementia related genes in the harbor porpoise.

Gene Probes	Neurological Diseases	Associated Neuropathology	Harbor Porpoise (qPCR)		Human (BioGPS)	
			Pc ^{V1} :CE	Fc:CE	Pc:CE	PreFc:CE
<i>APP</i> [34]	AD	A β ⁺ plaques	1.41 \pm 0.34	2.88 \pm 0.56 ^{$p < 0.0001$}	1.73	4.20
<i>PSEN1</i> [35]	AD	A β ⁺ plaques	1.23 \pm 0.02	1.33 \pm 0.03	7.48	7.56
<i>PSEN2</i> [36]	AD	A β ⁺ plaques	0.66 \pm 0.03	0.79 \pm 0.01	1.30	1.46
<i>GRN</i> [37]	FTLD	progranulin loss	1.38 \pm 0.02	1.96 \pm 0.04	1.24	1.42
<i>MAPT</i> [38]	Tauopathies	NFTs	1.52 \pm 0.07	2.40 \pm 0.14 ^{$p = 0.0134$}	4.08	7.24
<i>TARBDP</i> [39]	TDP-43 proteinopathies	IC	1.21 \pm 0.01	1.95 \pm 0.04	1.40	2.28
<i>C9orf72</i> [39]	ALS and FTD	IC	1.22 \pm 0.09	1.66 \pm 0.09	1.03	0.96

A β : amyloid beta; AD: Alzheimer's disease; ALS: amyotrophic lateral sclerosis; CE: cerebellum (baseline); Fc: frontal cortex; FTD: frontotemporal dementia; FTLD: frontotemporal lobar degeneration; IC: intracytoplasmic inclusions; Pc^{V1}: visual cortex; PreFc: prefrontal cortex.

2.4. Neuropathology

Gross examination of the left-brain hemisphere demonstrated leptomenigeal congestion and cerebral edema characterized by cortical gyral widening and sulcal effacement. The Ctx, CE, midbrain (Mid) and brainstem (Bs) were intact. The external examination revealed a normal gyral configuration without evidence of contusions or hemorrhage, cystic degeneration or xanthochromic discoloration (Figure 1A,B). The cerebrum was sectioned in the coronal plane. The cortical ribbon was of normal thickness and displayed appropriate gray-white matter demarcation without gross dysplasia, heterotopia or laminar necrosis. The subcortical white matter was congested, and the deep nuclei were symmetrical without infarction, hemorrhage or mass lesions. The cerebellum and brainstem had a normal gross architecture without infarction or lesions (Figure 1C). For comparison, examples of

normal cetacean gross neuroanatomy can be seen in brain atlases (see the Methods section). Diffuse-type phospho-TDP-43 CI were observed throughout the Crtx, Mid and Bs (Figure 2). TDP-43 CI were predominantly found in the perikaryon of neurons in the Crtx cortical layers II–VI. The occipital cortex (Oc) was negative for TDP-43 CI (Figure 2F, Table 3). In the hippocampus (Hipp), AD-type changes such as Hirano bodies [40], granulovacuolar degeneration bodies (GVBs) [41], intracellular tangles, ghost tangles and dense-core plaques [42] were present (Figure 3). Microtubule-associated protein 2 (MAP2) immunostaining highlighted degenerated neurons in the Cornu Ammonis areas of the Hipp and the Fc (Figure 3M,N). A β ⁺ plaques and intraneuronal staining was observed in all brain regions analyzed in this study (Figure 3O, Table 3). Moderate numbers of the A β ⁺ diffused and dense core plaques were wide-spread and varied in size (Figure 3P–R). Sequestosome 1 (P62/SQSTM1) staining was found in brain regions involved in the progression and neuropathological staging of AD and the CE (Table 3). P62/SQSTM1 staining was not observed in the Med, Pons, temporal cortex (Tc), Oc or Pc (Table 3). Hippocampal CA2 neurons, responsible for the formation of social memory, had numerous argyrophilic-, TDP-43⁺, A β ⁺, P62/SQSTM1⁺ intraneuronal inclusions and A β ⁺ plaque deposition (Figure 3S–V). These data suggest that the harbor porpoise can develop TDP-43 proteinopathy with co-current AD neuropathological changes.

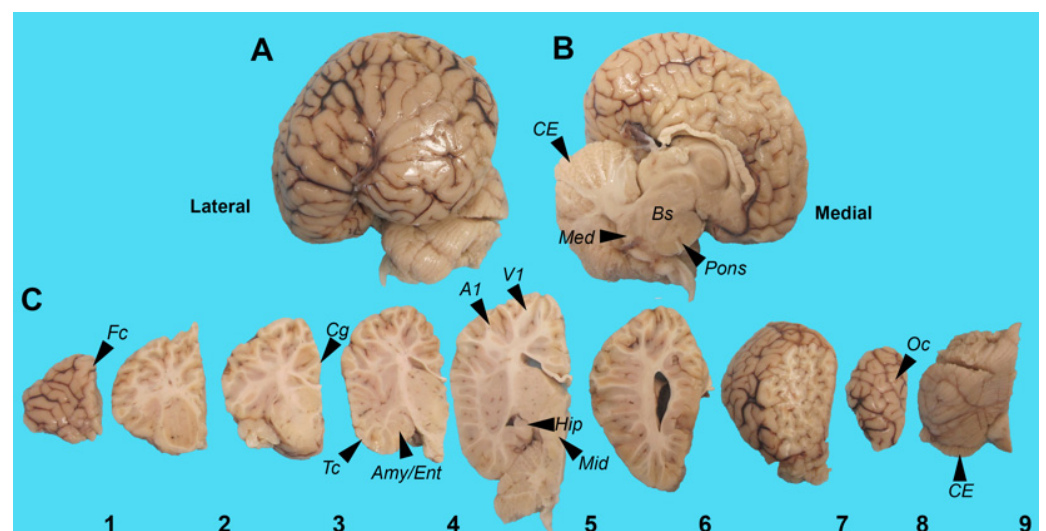


Figure 1. Gross examination of the harbor porpoise brain. Gross examination was performed on the left hemisphere of a beach harbor porpoise (*Phocoena phocoena*; IFAW12-206 Pp). (A) Lateral view of intact cerebrum and cerebellum. (B) Medial view of intact cerebrum, cerebellum (CE) and brainstem (Bs) containing the Pons and the medulla oblongata (Med). (C) Coronal sections of cerebrum (1 to 8 left to right) and detached cerebellum (9). Tissue samples were taken for histopathological analysis: 1: frontal cortex (Fc); 3: cingulate cortex (Cg); 4: amygdala (Amy), entorhinal cortex (Ent) and Temporal cortex (Tc); 5: hippocampus (Hipp), midbrain (Mid) and two gyri of the parietal cortex (Pc): auditory (A1) and visual cortex (V1). 8: occipital cortex (Oc) 9: CE.

Table 3. Histological results for brain tissue examined from a beached harbor porpoise exposed to BMAA.

Brain Regions	TDP-43 pSer 409/410	β -Amyloid 1–16 (clone 6E10)	P62/SQSTM1	SM: Argyrophilic Neurons and Plaques
Amy	+	+	+	+
CE	(–)/+	+	++	+
Cg	+	+	(–)	+
Ent	+	+	+	+
Fc	+	+	–/+	+

Table 3. Cont.

Brain Regions	TDP-43 pSer 409/410	β -Amyloid 1–16 (clone 6E10)	P62/SQSTM1	SM: Argyrophilic Neurons and Plaques
Hipp	+	+	+	+
Med	+	+	(–)	+
Mid	+	+	(–)	+
Oc	(–)	+	(–)	+
Pc ^{A1}	+	+	(–)	+
Pons	+	+	(–)	+

(–): negative; –/+ : sparse; +: positive; SM: Sevier M \ddot{u} nger; P62/SQSTM1: sequestosome 1.

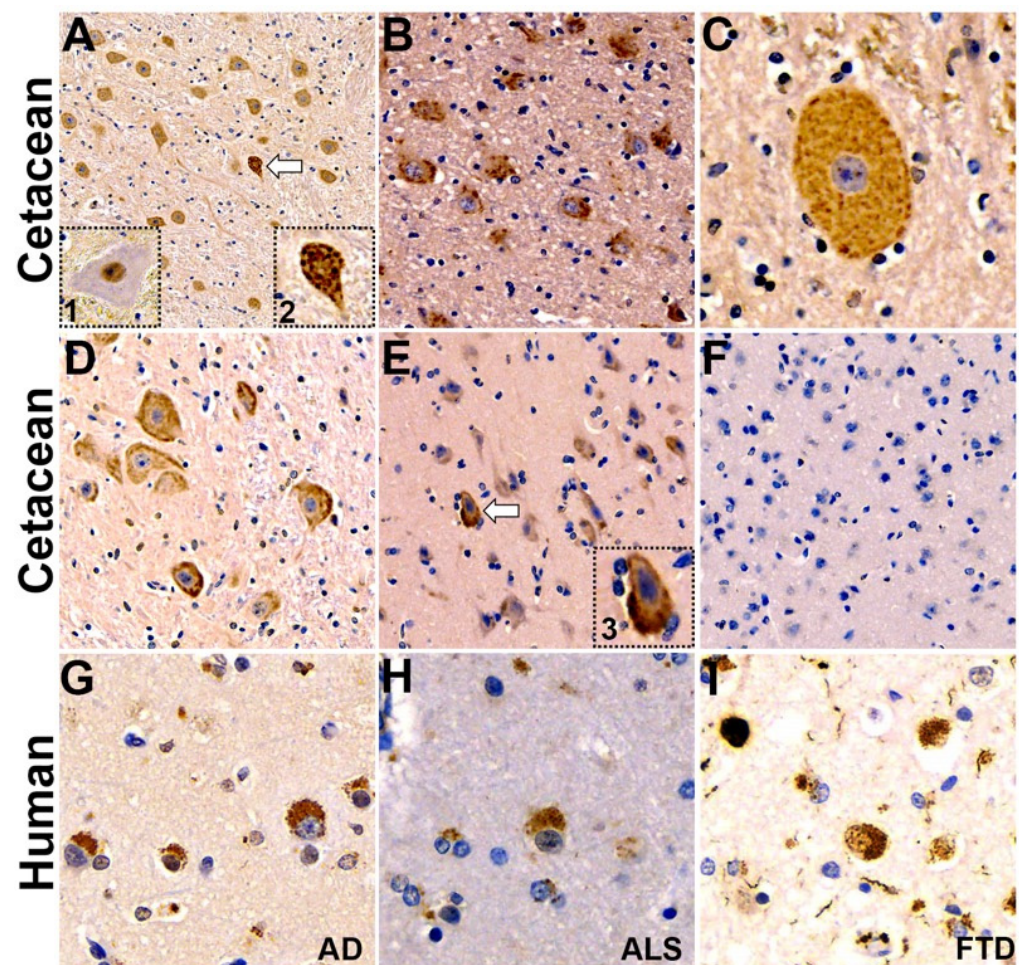


Figure 2. Comparative TDP-43 proteinopathy in the brain of a harbor porpoise exposed to the cyanobacterial toxin BMAA. Pathological diffused type cytoplasmic inclusions (CI) of TDP-43 were observed throughout the harbor porpoise brain. (A) medulla oblongata (Med); arrow indicates a neuron with severe density of TDP-43 CI. Inserts depict higher magnification images of neurons with normal (dotted box 1; from dolphin brain; low BMAA exposure) and pathological (dotted box 2; from harbor porpoise brain) expression of TDP-43. (B,C) Low- and high-magnification images of neurons in the pons region of brainstem. Images of neurons in the midbrain (Mid) (D) and frontal cortex (Fc) neurons in layers II–VI (E) that have TDP-43 CI. A higher-magnification image of a neuron in the Fc with is severe density of TDP-43 CI (arrow) depicted inset (dotted box 3). (F) TDP-43 CI were not observed in the occipital cortex (Oc). (G–H) TDP-43 CI observed in the Ctx of individuals with end stage Alzheimer’s disease (AD), amyotrophic lateral sclerosis (ALS) and frontal temporal dementia (FTD). Magnification: 10 \times (A); 20 \times (B–F); 60 \times (C); 40 \times (D–I); Inserts 1–3 (40 \times).

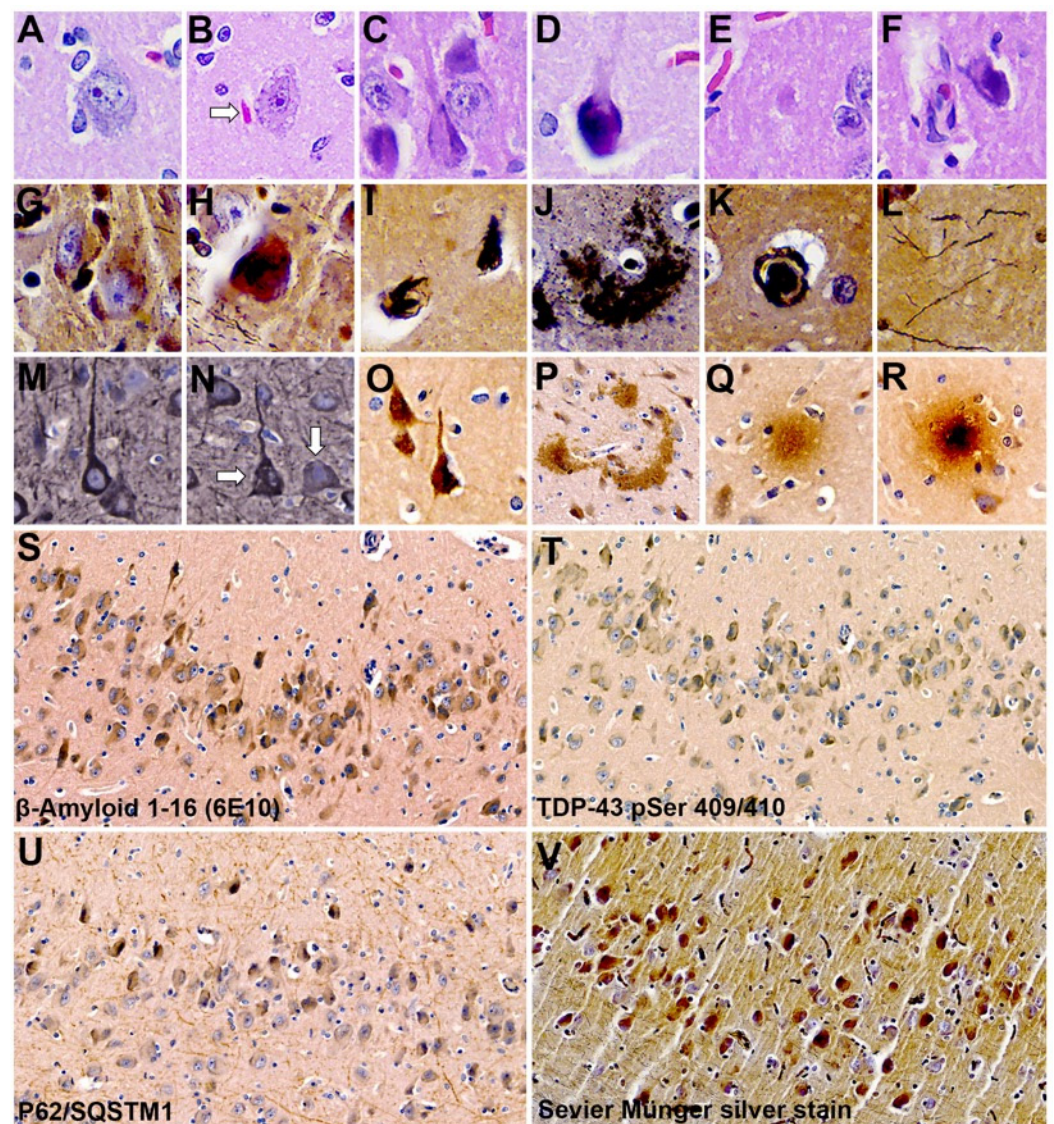


Figure 3. Alzheimer’s disease-like changes in a harbor porpoise exposed to the cyanobacterial toxin BMAA. H&E stains of the hippocampal pyramidal layers (A–E). Normal hippocampal pyramidal neuron (A), pyramidal neuron exhibiting granulo-vacuolar degeneration adjacent to a Hirano body (arrow) (B). Pyramidal neurons with the classic “flame-shaped” intracellular tangle (C). Pyramidal neuron with a globose tangle (D). Eosinophilic and plaques (E,F). Modified silver stains highlight argyrophilic intracellular inclusions (G,H), ghost tangles (I), diffuse plaques (J), a dense-core plaque (K) and neuropil threads (L). MAP2 immunostains highlight normal (M) and degenerative pyramidal neurons (N, arrows) in the frontal cortex. A β immunostains demonstrate an A β ⁺ neuron (O), diffuse plaques (P) and dense-core plaques (Q,R) in the entorhinal cortex and hippocampus. Motic digital scans of CA2 hippocampal fields immunoprobed with A β 6E10 (S), pathogenic TDP-43 pSer 409/410 (T), P62/sequestosome-1 (P62/SQSTM1) (U) and Sevier Mûnger silver stain (V). Magnification: 40 \times (A–R); 20 \times (S–V).

3. Discussion

Climate change, nutrient pollution and industrial waste are increasing the numbers of harmful cyanobacterial blooms (HCBs) [43,44]. HCBs produce cyanotoxins which can have wide-ranging effects on marine life, public health and the economy [45]. The impact of HCBs can vary depending on the region [46]. However, the harmful effects of some cyanotoxins, termed “slow toxins”, can manifest neurological symptoms in an individual decade after exposure [18]. Here, we examined the potential impact of cyanotoxin exposure

on a harbor porpoise, a species under increased metabolic stress due to their size, making them especially vulnerable to toxicity and mortality [47,48]. We detected BMAA, a neurotoxin produced by cyanobacteria, in the brain at concentrations comparable to individuals with AD, ALS and ALS/PDC [20,29]. We also detected two BMAA structural isomers: 2,4-DAB and AEG. We examined samples taken from two adjacent cortical gyri in the parietal cortex and did not observe a difference in BMAA or 2,4-DAB concentrations, but we did observe a difference in AEG. In vitro models have shown that all three compounds have different mechanisms of neurotoxicity [49]. Thus, the combined neurotoxic effects of all three compounds may be underestimated. More studies are needed to understand the regional distribution, differential concentrations and additive or synergistic effects of BMAA and BMAA isomers [50,51].

We also show here that the harbor porpoise express genes that are involved in the pathogenesis of AD and TDP-43 proteinopathies. Expression levels were highest in the frontal cortex and consisted of genes involved in the deposition of $A\beta^+$ plaques, NFTs and TDP-43 CI. The amyloid- β precursor protein (*APP*) was the most highly expressed gene and was accompanied by $A\beta^+$ deposits and plaques throughout the brain. In our analysis, we did not evaluate if mutations were present in the genes analyzed. However, the similarities in the differential expression of genes in the cortex versus the cerebellum suggest these genes may contribute to the development of neuropathology in the harbor porpoise as they do in humans. These findings along with previous studies from our group support the need for further research into understanding the impact of gene and cyanotoxin interactions on the cetacean brain [6].

BMAA exposure is a strong risk factor in the development of TDP-43 proteinopathy [52]. In non-human primates and rodents, BMAA exposure increases the deposition of TDP-43 cytoplasmic inclusions [23,25]. The co-occurrence of TDP-43 proteinopathy has been shown to increase the onset, severity and progression of AD [53]. Pathological TDP-43 causes greater atrophy of the hippocampus in AD, a brain region responsible for learning and memory [54]. The presence of TDP-43 CI is also a pathological hallmark of diseases such as ALS, FTD and limbic-predominant age-related TDP-43 encephalopathy (LATE) [55,56]. Here, we observed TDP-43 CI throughout the brain of a harbor porpoise exposed to BMAA. TDP-43 CI were found in the cerebral cortex, hippocampus and brainstem similar to the distribution reported in ALS/PDC [57]. Additional studies are necessary to understand the link between BMAA exposure, TDP-43 proteinopathies and if lesions are primary or secondary hallmarks of a neurodegenerative phenotype in the harbor porpoise.

We observed intraneuronal staining of P62/sequestosome 1 (P62/SQSTM1) a marker of autophagy of misfolded proteins. In AD, P62/SQSTM1 is associated with the early phases of NFT development [58]. Mutations in P62/SQSTM1 have been associated with ALS [59]. P62/SQSTM1 immunoreactivity was observed in neurons of brain regions implicated in the clinical progression of AD. The presence of TDP-43 CI, P62/SQSTM1, $A\beta$ and NFTs in CA2 hippocampal neurons, a region responsible for social memory, suggest neurotoxicity in the development of a progressive neurodegenerative disease [60,61]. Further studies are needed to examine other protein markers related to neurodegenerative disease in order to better understand the heterogeneity of pathology in the harbor porpoise.

Here, we also show two neuropathological hallmarks of AD: $A\beta^+$ plaques and NFTs. $A\beta^+$ plaques were observed throughout the brain regions analyzed and its immunoreactivity was robust using the β -Amyloid clone 6E10 antibody. NFTs were also widespread, consisting of pre-, mature and ghost or tombstone tangles similar to those observed in the common dolphin [6]. However, NFTs were identified in the harbor porpoise brain using Sevier Munger silver staining due to the negative immunoreactivity to AT8 (phospho-tau at serine 202, threonine 205) and the AT180 (phospho-tau at threonine 231) antibody that was reported by Vacher et al. [10]. These findings suggest other tau phospho-sites may be involved in the disease process in the harbor porpoise. Additional research is needed to delineate the phosphorylated tau sites involved in NFT formation in the brain of the harbor porpoise.

HCBs produce a number of cyanotoxins that affect the nervous system [62]. Experimental models have shown that the co-exposures to cyanobacterial toxins can be synergistic [63–67]. Compounds concentrated in the marine food web like methylmercury that has been shown to have synergistic effects with BMAA should also be considered when evaluating neurotoxicity in cetaceans [6,51,68,69]. Furthermore, infectious disease agents such as herpesvirus, morbillivirus, *Brucella ceti* and prions that can contribute to neurodegeneration in cetaceans should be considered as a co-morbidity with cyanotoxin exposures [8,11,46,70–73]. Future studies will be needed to assess the synergistic effects of cyanotoxin exposures and co-current neurological diseases on triggering TDP-43 and AD pathology.

4. Conclusions

The cyanotoxins BMAA, AEG and 2,4-DAB, were detected in the brain of a beached harbor porpoise. The harbor porpoise also displayed severe TDP-43 proteinopathy with AD-type neuropathological changes. These findings further support the development of a neurodegenerative phenotype in cetaceans and a potential causative link to chronic cyanotoxin exposure.

5. Materials and Methods

5.1. Harbor Porpoise Brain

A female subadult harbor porpoise (*Phocoena phocoena*) found beached in Massachusetts in March of 2012 was examined in this study. Physical assessments performed on-site by the stranding response team determined the harbor porpoise was in poor health and should be subsequently euthanized. The harbor porpoise (ID: IFAW 12-206 Pp) was not euthanized for this research study. A necropsy was performed the next day at the Woods Hole Oceanographic Institute Marine Research Facility (WHOI MRF) and the International Fund for Animal Welfare (IFAW). The age class of IFAW 12-206 Pp was estimated as described in Geraci et al. [74]. For neurotoxicological analysis, the brain was removed and the right hemisphere was frozen. The contralateral brain hemisphere was fixed in 10% buffered formalin. After preservation, the whole brain was shipped to the University of Miami Brain Endowment Bank (UMBEB) for further analysis. Upon receipt, frozen parietal cortex-visual cortex area 1 (Pc^{V1}), frontal cortex (Fc) and the cerebellar hemisphere (CE) were dissected for qPCR analysis. Twelve brain regions were sampled from the left hemisphere for neuropathological evaluation: amygdala (Amy); CE; cingulate gyrus (Cg); entorhinal cortex (Ent); hippocampus (Hipp); medulla oblongata (Med); occipital cortex (Oc); parietal cortex (Pc^{A1}), Pc^{V1} , pontine (Pons); temporal cortex (Tc). Brain atlases by Breathnach and Goldby [75] and Marino et al. [76] were used for the identification of harbor porpoise neuroanatomy. The Michigan State University Brain Biodiversity Bank Dolphin Atlas was also used as another reference for normal cetacean neuroanatomy (<https://brains.anatomy.msu.edu/brains/dolphin/index.html>) accessed on 29 December 2023. Experiments in this manuscript were approved by the National Oceanic Atmospheric Administration (NOAA) Southeast Region Stranding Program and NOAA Fisheries Service. The University of Miami Institutional Animal Care and Use Committee (IACUC) reviewed and authorized this study before receiving brain specimens. The handling of the harbor porpoise tissues satisfies the requirements of the Marine Mammal Protection Act pursuant to 50 CFR 216.22.

5.2. HPLC/FD

High-performance liquid chromatography with fluorescence detection (HPLC-FD) as previously described in Davis et al. 2019 was used to measure BMAA in 150 mg of porpoise cortical brain tissue [7,29]. Briefly, BMAA was separated from two structural isomers 2,4-diaminobutyric acid (2,4-DAB) and (N-(2-aminoethyl)glycine (AEG) using reverse-phase elution on a 1525 Binary HPLC pump and a 717 autosampler (Waters Corp., Milford, MA, USA). Analytes of interests were separated at 33.0 min (2,4-DAB), 31.1 min (BMAA) and

29.6 min for (AEG). The detection of analytes utilized a 2475 Multi k-Fluorescence Detector (Waters Corp., USA) with excitation/emission at 250/395 nm, respectively. Replicate measurements ($n = 4-5$) were performed for each brain region (Pc^{A1} and Pc^{V1}) and compared to control samples containing known amounts of an L-BMAA standard (Sigma-Aldrich, St. Louis, MO, USA). The limit of detection and the limit of quantification for our analysis were 2.7 ng/mL and 7.0 ng/mL, respectively.

5.3. qPCR Analysis

Brain tissues samples from Pc^{V1} , Fc and CE (100 mg) were dissected to extract the total RNA using an RNeasy Lipid Tissue Mini Kit and DNase I on-column treatment (Qiagen Inc., Germantown, MD, USA). RNA concentration ($\mu\text{g}/\mu\text{L}$) and quality (RIN) were measured for each sample using a NanoDrop 2000 Spectrophotometer (Thermo Fisher Scientific, Waltham, MA, USA) and an Agilent 2100 Bioanalyzer (Agilent Technologies Inc., Santa Clara, CA, USA). In this study, high-quality RNA samples were used for IFAW 12-206 Pp, which averaged a RIN of 9.7 out of 10. Total RNA (5 μg) and a High Capacity Reverse Transcription Kit (Thermo Fisher Scientific, Waltham, MA, USA) was used to create complementary DNA (cDNA) libraries for each brain region of interest. A custom dolphin PCR assay containing seven genes (*APP*, *PSEN1*, *PSEN2*, *MAPT*, *GRN*, *TARDBP* and *C9orf72*) involved in the development of AD and TDP-43 proteinopathies were created to measure gene expression using a TaqMan Universal PCR Master Mix on a QuantStudio® 6 Flex Real-Time PCR System (Thermo Fisher Scientific, Waltham, MA, USA) [6]. Gene primers were designed based on the *T. truncatus* genome turTur1, in combination with a limited sequence of *D. delphis* (ncbi.nlm.nih.gov/bioproject/421547, accessed on 29 December 2023) (Table S1) [77]. *RPS9* (40S ribosomal protein S9), a very stable gene in cetaceans was used to normalize gene expression [78]. The following conditions were used to amplify 100 ng of cDNA: 120 s at 50 °C, 600 s at 95 °C, then 40 cycles: 15 s at 95 °C and 60 s at 60 °C. Data files were imported into ExpressionSuite Software v1.0.4 (Applied Biosystems, Foster City, CA, USA) to analyze relative expression across all plates using the comparative *Ct* method [79]. After data normalization, fold changes for Pc^{V1} and Fc were calculated using the cerebellum as a calibrator. Brain-region-specific gene expression values for the harbor porpoise were compared to analogous brain regions in humans (parietal cortex, prefrontal cortex and cerebellum) using the BioGPS database (Scripps Research Institute, San Diego, CA, USA). The following NCBI Gene IDs were evaluated in BioGPS: *APP* (351), *PSEN1* (5663), *PSEN2* (5664), *MAPT* (4137), *GRN* (2896), *TARDBP* (23435) and *C9orf72* (203228); <http://biogps.org/>; accessed on 27 December 2023 [80].

5.4. Immunohistochemistry and Digital Pathology

Formalin-fixed paraffin-embedded brain tissue sections (7 μm) were prepared using a Leica microtome (Leica Biosystems, Deer Park, IL, USA) and mounted to positive charge slides as previously described [6]. Tissue sections were dehydrated, deparaffinized and placed into 3% hydrogen peroxide for 10 min to inhibit endogenous peroxidase activity. Antigen retrieval was performed by immersing brain tissue sections into heated 10 mM citric acid (pH 6.0) for 30 min followed by cooling in deionized water. For Tau AT8 immunostaining, slides were submerged into formic acid (Sigma-Aldrich, St. Louis, MO, USA) for 5 min to perform antigen retrieval. Following antigen retrieval, 5% goat serum (Vector Laboratories, Newark, CA, USA) was applied to tissues sections for 20 min to block nonspecific antibody binding. The following primary antibodies were incubated on tissue sections overnight at 4 °C: β -Amyloid 1–16 (6E10; 1.25 $\mu\text{g}/\text{mL}$; BioLegend, San Diego, CA, USA), Tau AT8 (pSer202/Thr205; 0.4 $\mu\text{g}/\text{mL}$; Thermo Fisher Chemicals, Waltham, MA, USA), TDP-43 (pSer409/410; 1.0 $\mu\text{g}/\text{mL}$; Cosmo Bio, Carlsbad, CA, USA), TARDBP (A01; 1.0 $\mu\text{g}/\text{mL}$; Abnova, Walnut, CA, USA), P62/SQSTM1 (1.0 $\mu\text{g}/\text{mL}$; Abnova, Walnut, CA, USA) and MAP2 (0.5 $\mu\text{g}/\text{mL}$; Sigma, St. Louis, MO, USA) in phosphate-buffered saline (PBS). The next day, goat-anti-rabbit IgG or horse-anti-mouse IgG biotinylated secondary antibodies were applied to brain sections (15 $\mu\text{g}/\text{mL}$; Vector Laboratories, Newark, CA, USA)

for 60 min before adding the avidin–biotin complex for an additional 60 min (1:200, ABC; Vector Laboratories, Newark, CA, USA). To visualize the reaction, 3,3'-diaminobenzidine or DAB (Millipore Sigma, Burlington, VT, USA) was added to brain sections for 10 min. Postmortem brain tissue sections from AD patients were used as positive pathology controls. Archived formalin-fixed autopsy cerebral cortex samples from brain donors with intermediate to high AD (W/F/84; PMI: 16.3 h), ALS (W/M/63; PMI: 33.3 h) and FTD (W/F/68; PMI: 29.6 h) were used for comparative TDP-43 neuropathology. The donated human tissues were acquired from the University of Miami Brain Endowment Bank, an NIH NeuroBioBank under the IRB 19920348. A common dolphin (ID: IFAW 12-228 Dd) with a low BMAA tissue concentration was used to demonstrate non-pathogenic TDP-43 nuclear protein expression [7]. Immunostaining in the absence of the primary antibody was used as a negative control. Sevier Munger silver staining of harbor porpoise tissue sections was performed by AML Laboratories using an American MasterTech special kit (American MasterTech, Lodi, CA, USA) [81]. A 40 \times digital scan of each slide was generated using an EasyScan Pro 6 (Motic, Schertz, TX, USA) and exported to ObjectiveViewTM (Objective Pathology, Halton Hills, ON, Canada) and FIJI ImageJ VER2.00-rc-69/1.52p (National Institute of Health, USA) for analysis. A 2 \times 5 grid totaling 1 mm² was applied to the cortical layers II–VI, the CA2 field of the Hipp and the Purkinje cell layer of the CE. A semiquantitative scale was used to define pathology: (–) negative; (–/+) rare or sparse; (+) positive.

5.5. Statistical Analyses

Two-way ANOVA with Šidak's multiple comparison test and Pearson r tests with a significance level of $\alpha = 0.05$ were performed using Prism Version 9.5.1 (528) (Graph Pad, Boston, MA, USA). The normality of data was determined using the Shapiro–Wilk test. Data are presented as the mean \pm standard error.

Supplementary Materials: The following supporting information can be downloaded at: <https://www.mdpi.com/article/10.3390/toxins16010042/s1>, Table S1: Primer designs based on *T. truncatus* and *D. delphis* sequence.

Author Contributions: Conceptualization: D.A.D.; methodology: S.P.G., D.J.B., R.T.V. and D.A.D.; software: S.P.G. and D.A.D.; validation: S.P.G., D.J.B., T.M.C. and R.T.V.; formal analysis: S.P.G. and D.A.D.; investigation: S.P.G., R.T.V. and D.A.D.; resources: S.P.G., R.T.V. and D.A.D.; data curation: S.P.G. and D.A.D.; writing—original draft preparation: D.A.D.; writing—review and editing: S.P.G., D.J.B., T.M.C., R.T.V. and D.A.D.; visualization: S.P.G. and D.A.D.; supervision: D.A.D.; project administration: S.P.G. and D.A.D.; funding acquisition: D.A.D. All authors have read and agreed to the published version of the manuscript.

Funding: This research was funded by the Herbert W. Hoover Foundation by a research grant provided to David A. Davis (#GR012556; 2018 to 2019).

Institutional Review Board Statement: Postmortem human brain biospecimens were obtained from the University of Miami Brain Endowment Bank (IRB 19920348). The beached harbor porpoise evaluated in this study was collected under a federal permit approved by the National Ocean and Atmospheric Administration (NOAA) as a part of the Stranding Agreement for the Marine Mammal Health and Stranding Response Act. The experiments in this paper were sanctioned by the NOAA Southeast Region Stranding Program and National Marine Fisheries Service. The University of Miami Institutional Animal Care and Use Committee (IACUC) reviewed and approved this study preceding the receipt of the harbor porpoise biospecimens. The experiments and handling of the harbor porpoise brain tissues satisfied the requirements of the Marine Mammal Protection Act pursuant to 50 CFR 216.22.

Informed Consent Statement: Not applicable.

Data Availability Statement: All data are present in the article.

Acknowledgments: We would like to acknowledge the support of the International Fund for Animal Welfare for porpoise biospecimen collection. We thank Kiyu Mondo for assistance with HPLC-FD testing. We are grateful for Angela M. Amatruda and her team at AML Laboratories, St. Augustine, Florida, for performing silver staining. We are thankful for the help of Patricia Luecasy with H&E staining. We thank the University of Miami Brain Endowment Bank, a NIH NeuroBioBank, for providing archived donated postmortem human brain tissues used as technical and comparative controls for this study.

Conflicts of Interest: The authors declare no conflicts of interest.

References

1. Bruck, J.N. Decades-long social memory in bottlenose dolphins. *Proc. Biol. Sci.* **2013**, *280*, 20131726. [[CrossRef](#)] [[PubMed](#)]
2. Cairnson, O. External measures of cognition. *Front. Hum. Neurosci.* **2011**, *5*, 108. [[CrossRef](#)]
3. Hof, P.R.; Chavis, R.; Marino, L. Cortical complexity in cetacean brains. *Anat. Rec. Discov. Mol. Cell Evol. Biol.* **2005**, *287*, 1142–1152. [[CrossRef](#)]
4. Dell, L.A.; Patzke, N.; Spocter, M.A.; Siegel, J.M.; Manger, P.R. Organization of the sleep-related neural systems in the brain of the harbour porpoise (*Phocoena phocoena*). *J. Comp. Neurol.* **2016**, *524*, 1999–2017. [[CrossRef](#)]
5. Kruger, L. Edward Tyson's 1680 account of the 'porpess' brain and its place in the history of comparative neurology. *J. Hist. Neurosci.* **2003**, *12*, 339–349. [[CrossRef](#)] [[PubMed](#)]
6. Davis, D.A.; Garamszegi, S.P.; Banack, S.A.; Dooley, P.D.; Coyne, T.M.; McLean, D.W.; Rotstein, D.S.; Mash, D.C.; Cox, P.A. BMAA, Methylmercury, and Mechanisms of Neurodegeneration in Dolphins: A Natural Model of Toxin Exposure. *Toxins* **2021**, *13*, 697. [[CrossRef](#)]
7. Davis, D.A.; Mondo, K.; Stern, E.; Annor, A.K.; Murch, S.J.; Coyne, T.M.; Brand, L.E.; Niemeyer, M.E.; Sharp, S.; Bradley, W.G.; et al. Cyanobacterial neurotoxin BMAA and brain pathology in stranded dolphins. *PLoS ONE* **2019**, *14*, e0213346. [[CrossRef](#)]
8. Pintore, M.D.; Mignone, W.; Di Guardo, G.; Mazzariol, S.; Ballardini, M.; Florio, C.L.; Gorla, M.; Romano, A.; Caracappa, S.; Giorda, F.; et al. Neuropathologic Findings in Cetaceans Stranded in Italy (2002–2014). *J. Wildl. Dis.* **2018**, *54*, 295–303. [[CrossRef](#)]
9. Sips, G.J.; Chesik, D.; Glazenburg, L.; Wilschut, J.; De Keyser, J.; Wilczak, N. Involvement of morbilliviruses in the pathogenesis of demyelinating disease. *Rev. Med. Virol.* **2007**, *17*, 223–244. [[CrossRef](#)]
10. Vacher, M.C.; Durrant, C.S.; Rose, J.; Hall, A.J.; Spires-Jones, T.L.; Gunn-Moore, F.; Dagleish, M.P. Alzheimer's disease-like neuropathology in three species of oceanic dolphin. *Eur. J. Neurosci.* **2023**, *57*, 1161–1179. [[CrossRef](#)]
11. Di Guardo, G. Alzheimer's disease, cellular prion protein, and dolphins. *Alzheimers Dement.* **2018**, *14*, 259–260. [[CrossRef](#)]
12. Reif, J.S.; Schaefer, A.M.; Bossart, G.D. Atlantic Bottlenose Dolphins (*Tursiops truncatus*) as A Sentinel for Exposure to Mercury in Humans: Closing the Loop. *Vet. Sci.* **2015**, *2*, 407–422. [[CrossRef](#)]
13. Tilbury, K.L.; Stein, J.E.; Meador, J.P.; Krone, C.A.; Chan, S.L. Chemical contaminants in harbor porpoise (*Phocoena phocoena*) from the north Atlantic coast: Tissue concentrations and intra- and inter-organ distribution. *Chemosphere* **1997**, *34*, 2159–2181. [[CrossRef](#)]
14. Van de Vijver, K.I.; Holsbeek, L.; Das, K.; Blust, R.; Joiris, C.; De Coen, W. Occurrence of perfluorooctane sulfonate and other perfluorinated alkylated substances in harbor porpoises from the Black Sea. *Environ. Sci. Technol.* **2007**, *41*, 315–320. [[CrossRef](#)]
15. Banack, S.A.; Johnson, H.E.; Cheng, R.; Cox, P.A. Production of the neurotoxin BMAA by a marine cyanobacterium. *Mar. Drugs* **2007**, *5*, 180–196. [[CrossRef](#)]
16. Cox, P.A.; Banack, S.A.; Murch, S.J.; Rasmussen, U.; Tien, G.; Bidigare, R.R.; Metcalf, J.S.; Morrison, L.F.; Codd, G.A.; Bergman, B. Diverse taxa of cyanobacteria produce beta-N-methylamino-L-alanine, a neurotoxic amino acid. *Proc. Natl. Acad. Sci. USA* **2005**, *102*, 5074–5078. [[CrossRef](#)]
17. Cox, P.A.; Kostrzewa, R.M.; Guillemin, G.J. BMAA and Neurodegenerative Illness. *Neurotox. Res.* **2018**, *33*, 178–183. [[CrossRef](#)]
18. Cox, P.A.; Sacks, O.W. Cycad neurotoxins, consumption of flying foxes, and ALS-PDC disease in Guam. *Neurology* **2002**, *58*, 956–959. [[CrossRef](#)]
19. Banack, S.A.; Murch, S.J.; Cox, P.A. Neurotoxic flying foxes as dietary items for the Chamorro people, Marianas Islands. *J. Ethnopharmacol.* **2006**, *106*, 97–104. [[CrossRef](#)]
20. Murch, S.J.; Cox, P.A.; Banack, S.A.; Steele, J.C.; Sacks, O.W. Occurrence of beta-methylamino-L-alanine (BMAA) in ALS/PDC patients from Guam. *Acta Neurol. Scand.* **2004**, *110*, 267–269. [[CrossRef](#)]
21. Mimuro, M.; Yoshida, M.; Kuzuhara, S.; Kokubo, Y. Amyotrophic lateral sclerosis and parkinsonism-dementia complex of the Hohara focus of the Kii Peninsula: A multiple proteinopathy? *Neuropathology* **2018**, *38*, 98–107. [[CrossRef](#)]
22. Geser, F.; Winton, M.J.; Kwong, L.K.; Xu, Y.; Xie, S.X.; Igaz, L.M.; Garruto, R.M.; Perl, D.P.; Galasko, D.; Lee, V.M.; et al. Pathological TDP-43 in parkinsonism-dementia complex and amyotrophic lateral sclerosis of Guam. *Acta Neuropathol.* **2008**, *115*, 133–145. [[CrossRef](#)]
23. Davis, D.A.; Cox, P.A.; Banack, S.A.; Lecusay, P.D.; Garamszegi, S.P.; Hagan, M.J.; Powell, J.T.; Metcalf, J.S.; Palmour, R.M.; Beierschmitt, A.; et al. L-Serine Reduces Spinal Cord Pathology in a Vervet Model of Preclinical ALS/MND. *J. Neuropathol. Exp. Neurol.* **2020**, *79*, 393–406. [[CrossRef](#)]

24. Cox, P.A.; Davis, D.A.; Mash, D.C.; Metcalf, J.S.; Banack, S.A. Dietary exposure to an environmental toxin triggers neurofibrillary tangles and amyloid deposits in the brain. *Proc. Biol. Sci.* **2016**, *283*, 20152397. [[CrossRef](#)]
25. Yin, H.Z.; Yu, S.; Hsu, C.I.; Liu, J.; Acab, A.; Wu, R.; Tao, A.; Chiang, B.J.; Weiss, J.H. Intrathecal infusion of BMAA induces selective motor neuron damage and astrogliosis in the ventral horn of the spinal cord. *Exp. Neurol.* **2014**, *261*, 1–9. [[CrossRef](#)]
26. Hammerschlag, N.; Davis, D.A.; Mondo, K.; Seely, M.S.; Murch, S.J.; Glover, W.B.; Divoll, T.; Evers, D.C.; Mash, D.C. Cyanobacterial Neurotoxin BMAA and Mercury in Sharks. *Toxins* **2016**, *8*, 238. [[CrossRef](#)]
27. Mondo, K.; Hammerschlag, N.; Basile, M.; Pablo, J.; Banack, S.A.; Mash, D.C. Cyanobacterial neurotoxin beta-N-methylamino-L-alanine (BMAA) in shark fins. *Mar. Drugs* **2012**, *10*, 509–520. [[CrossRef](#)]
28. Brand, L.E.; Pablo, J.; Compton, A.; Hammerschlag, N.; Mash, D.C. Cyanobacterial blooms and the occurrence of the neurotoxin beta-N-methylamino-L-alanine (BMAA) in South Florida aquatic food webs. *Harmful Algae* **2010**, *9*, 620–635. [[CrossRef](#)]
29. Pablo, J.; Banack, S.A.; Cox, P.A.; Johnson, T.E.; Papapetropoulos, S.; Bradley, W.G.; Buck, A.; Mash, D.C. Cyanobacterial neurotoxin BMAA in ALS and Alzheimer’s disease. *Acta Neurol. Scand.* **2009**, *120*, 216–225. [[CrossRef](#)]
30. Garamszegi, S.P.; Banack, S.A.; Duque, L.L.; Metcalf, J.S.; Stommel, E.W.; Cox, P.A.; Davis, D.A. Detection of beta-N-methylamino-L-alanine in postmortem olfactory bulbs of Alzheimer’s disease patients using UHPLC-MS/MS: An autopsy case-series study. *Toxicol. Rep.* **2023**, *10*, 87–96. [[CrossRef](#)]
31. Berntzon, L.; Ronnevi, L.O.; Bergman, B.; Eriksson, J. Detection of BMAA in the human central nervous system. *Neuroscience* **2015**, *292*, 137–147. [[CrossRef](#)]
32. Meneely, J.P.; Chevallier, O.P.; Graham, S.; Greer, B.; Green, B.D.; Elliott, C.T. beta-methylamino-L-alanine (BMAA) is not found in the brains of patients with confirmed Alzheimer’s disease. *Sci. Rep.* **2016**, *6*, 36363. [[CrossRef](#)]
33. Montine, T.J.; Li, K.; Perl, D.P.; Galasko, D. Lack of beta-methylamino-L-alanine in brain from controls, AD, or Chamorro with PDC. *Neurology* **2005**, *65*, 768–769. [[CrossRef](#)]
34. O’Brien, R.J.; Wong, P.C. Amyloid precursor protein processing and Alzheimer’s disease. *Annu. Rev. Neurosci.* **2011**, *34*, 185–204. [[CrossRef](#)]
35. Kelleher, R.J., 3rd; Shen, J. Presenilin-1 mutations and Alzheimer’s disease. *Proc. Natl. Acad. Sci. USA* **2017**, *114*, 629–631. [[CrossRef](#)]
36. Cai, Y.; An, S.S.; Kim, S. Mutations in presenilin 2 and its implications in Alzheimer’s disease and other dementia-associated disorders. *Clin. Interv. Aging* **2015**, *10*, 1163–1172. [[CrossRef](#)]
37. Kuang, L.; Hashimoto, K.; Huang, E.J.; Gentry, M.S.; Zhu, H. Frontotemporal dementia non-sense mutation of progranulin rescued by aminoglycosides. *Hum. Mol. Genet.* **2020**, *29*, 624–634. [[CrossRef](#)]
38. Strang, K.H.; Golde, T.E.; Giasson, B.I. MAPT mutations, tauopathy, and mechanisms of neurodegeneration. *Lab. Investig.* **2019**, *99*, 912–928. [[CrossRef](#)]
39. Gendron, T.F.; Rademakers, R.; Petrucelli, L. TARDBP mutation analysis in TDP-43 proteinopathies and deciphering the toxicity of mutant TDP-43. *J. Alzheimers Dis.* **2013**, *33* (Suppl. S1), S35–S45. [[CrossRef](#)]
40. Mitake, S.; Ojika, K.; Hirano, A. Hirano bodies and Alzheimer’s disease. *Kaohsiung J. Med. Sci.* **1997**, *13*, 10–18.
41. Yamazaki, Y.; Matsubara, T.; Takahashi, T.; Kurashige, T.; Dohi, E.; Hiji, M.; Nagano, Y.; Yamawaki, T.; Matsumoto, M. Granulovacuolar degenerations appear in relation to hippocampal phosphorylated tau accumulation in various neurodegenerative disorders. *PLoS ONE* **2011**, *6*, e26996. [[CrossRef](#)] [[PubMed](#)]
42. Moloney, C.M.; Lowe, V.J.; Murray, M.E. Visualization of neurofibrillary tangle maturity in Alzheimer’s disease: A clinicopathologic perspective for biomarker research. *Alzheimers Dement.* **2021**, *17*, 1554–1574. [[CrossRef](#)]
43. Gobler, C.J. Climate Change and Harmful Algal Blooms: Insights and perspective. *Harmful Algae* **2020**, *91*, 101731. [[CrossRef](#)] [[PubMed](#)]
44. Heisler, J.; Glibert, P.; Burkholder, J.; Anderson, D.; Cochlan, W.; Dennison, W.; Gobler, C.; Dortch, Q.; Heil, C.; Humphries, E.; et al. Eutrophication and Harmful Algal Blooms: A Scientific Consensus. *Harmful Algae* **2008**, *8*, 3–13. [[CrossRef](#)] [[PubMed](#)]
45. Huisman, J.; Codd, G.A.; Paerl, H.W.; Ibelings, B.W.; Verspagen, J.M.H.; Visser, P.M. Cyanobacterial blooms. *Nat. Rev. Microbiol.* **2018**, *16*, 471–483. [[CrossRef](#)] [[PubMed](#)]
46. Hallegraeff, G.M.; Anderson, D.M.; Belin, C.; Bottein, M.Y.; Bresnan, E.; Chinain, M.; Enevoldsen, H.; Iwataki, M.; Karlson, B.; McKenzie, C.H.; et al. Perceived global increase in algal blooms is attributable to intensified monitoring and emerging bloom impacts. *Commun. Earth Environ.* **2021**, *2*, 117. [[CrossRef](#)]
47. Van den Heuvel-Greve, M.J.; van den Brink, A.M.; Kotterman, M.J.J.; Kwadijk, C.; Geelhoed, S.C.V.; Murphy, S.; van den Broek, J.; Heesterbeek, H.; Grone, A.; LL, I.J. Polluted porpoises: Generational transfer of organic contaminants in harbour porpoises from the southern North Sea. *Sci. Total Environ.* **2021**, *796*, 148936. [[CrossRef](#)] [[PubMed](#)]
48. Fenton, H.; Daoust, P.Y.; Forzan, M.J.; Vanderstichel, R.V.; Ford, J.K.; Spaven, L.; Lair, S.; Raverty, S. Causes of mortality of harbor porpoises *Phocoena phocoena* along the Atlantic and Pacific coasts of Canada. *Dis. Aquat. Organ.* **2017**, *122*, 171–183. [[CrossRef](#)]
49. Schneider, T.; Simpson, C.; Desai, P.; Tucker, M.; Lobner, D. Neurotoxicity of isomers of the environmental toxin L-BMAA. *Toxicol.* **2020**, *184*, 175–179. [[CrossRef](#)]
50. Martin, R.M.; Stallrich, J.; Bereman, M.S. Mixture designs to investigate adverse effects upon co-exposure to environmental cyanotoxins. *Toxicology* **2019**, *421*, 74–83. [[CrossRef](#)]
51. Rush, T.; Liu, X.; Lobner, D. Synergistic toxicity of the environmental neurotoxins methylmercury and beta-N-methylamino-L-alanine. *Neuroreport* **2012**, *23*, 216–219. [[CrossRef](#)] [[PubMed](#)]

52. Newell, M.E.; Adhikari, S.; Halden, R.U. Systematic and state-of the science review of the role of environmental factors in Amyotrophic Lateral Sclerosis (ALS) or Lou Gehrig's Disease. *Sci. Total Environ.* **2022**, *817*, 152504. [[CrossRef](#)]
53. Meneses, A.; Koga, S.; O'Leary, J.; Dickson, D.W.; Bu, G.; Zhao, N. TDP-43 Pathology in Alzheimer's Disease. *Mol. Neurodegener.* **2021**, *16*, 84. [[CrossRef](#)] [[PubMed](#)]
54. Wilson, A.C.; Dugger, B.N.; Dickson, D.W.; Wang, D.S. TDP-43 in aging and Alzheimer's disease—A review. *Int. J. Clin. Exp. Pathol.* **2011**, *4*, 147–155. [[PubMed](#)]
55. Nelson, P.T.; Dickson, D.W.; Trojanowski, J.Q.; Jack, C.R.; Boyle, P.A.; Arfanakis, K.; Rademakers, R.; Alafuzoff, I.; Attems, J.; Brayne, C.; et al. Limbic-predominant age-related TDP-43 encephalopathy (LATE): Consensus working group report. *Brain* **2019**, *142*, 1503–1527. [[CrossRef](#)]
56. De Boer, E.M.J.; Orié, V.K.; Williams, T.; Baker, M.R.; De Oliveira, H.M.; Polvikoski, T.; Silsby, M.; Menon, P.; van den Bos, M.; Halliday, G.M.; et al. TDP-43 proteinopathies: A new wave of neurodegenerative diseases. *J. Neurol. Neurosurg. Psychiatry* **2020**, *92*, 86–95. [[CrossRef](#)]
57. Hasegawa, M.; Arai, T.; Akiyama, H.; Nonaka, T.; Mori, H.; Hashimoto, T.; Yamazaki, M.; Oyanagi, K. TDP-43 is deposited in the Guam parkinsonism-dementia complex brains. *Brain* **2007**, *130*, 1386–1394. [[CrossRef](#)]
58. Kuusisto, E.; Salminen, A.; Alafuzoff, I. Early accumulation of p62 in neurofibrillary tangles in Alzheimer's disease: Possible role in tangle formation. *Neuropathol. Appl. Neurobiol.* **2002**, *28*, 228–237. [[CrossRef](#)]
59. Fecto, F.; Yan, J.; Vemula, S.P.; Liu, E.; Yang, Y.; Chen, W.; Zheng, J.G.; Shi, Y.; Siddique, N.; Arrat, H.; et al. SQSTM1 mutations in familial and sporadic amyotrophic lateral sclerosis. *Arch. Neurol.* **2011**, *68*, 1440–1446. [[CrossRef](#)]
60. Chevalyre, V.; Piskorowski, R.A. Hippocampal Area CA2: An Overlooked but Promising Therapeutic Target. *Trends Mol. Med.* **2016**, *22*, 645–655. [[CrossRef](#)]
61. Meira, T.; Leroy, F.; Buss, E.W.; Oliva, A.; Park, J.; Siegelbaum, S.A. A hippocampal circuit linking dorsal CA2 to ventral CA1 critical for social memory dynamics. *Nat. Commun.* **2018**, *9*, 4163. [[CrossRef](#)] [[PubMed](#)]
62. Metcalf, J.S.; Tischbein, M.; Cox, P.A.; Stommel, E.W. Cyanotoxins and the Nervous System. *Toxins* **2021**, *13*, 660. [[CrossRef](#)]
63. Al-Sammak, M.A.; Hoagland, K.D.; Cassada, D.; Snow, D.D. Co-occurrence of the cyanotoxins BMAA, DABA and anatoxin-a in Nebraska reservoirs, fish, and aquatic plants. *Toxins* **2014**, *6*, 488–508. [[CrossRef](#)]
64. Main, B.J.; Rodgers, K.J. Assessing the Combined Toxicity of BMAA and Its Isomers 2,4-DAB and AEG In Vitro Using Human Neuroblastoma Cells. *Neurotox. Res.* **2018**, *33*, 33–42. [[CrossRef](#)] [[PubMed](#)]
65. Violi, J.P.; Pu, L.; Pravadali-Cekic, S.; Bishop, D.P.; Phillips, C.R.; Rodgers, K.J. Effects of the Toxic Non-Protein Amino Acid β -Methylamino-L-Alanine (BMAA) on Intracellular Amino Acid Levels in Neuroblastoma Cells. *Toxins* **2023**, *15*, 647. [[CrossRef](#)] [[PubMed](#)]
66. Banack, S.A.; Caller, T.; Henegan, P.; Haney, J.; Murby, A.; Metcalf, J.S.; Powell, J.; Cox, P.A.; Stommel, E. Detection of cyanotoxins, beta-N-methylamino-L-alanine and microcystins, from a lake surrounded by cases of amyotrophic lateral sclerosis. *Toxins* **2015**, *7*, 322–336. [[CrossRef](#)] [[PubMed](#)]
67. Parsons, M.L.; Peccia, J.; Arnold, W. *Preliminary Report on Air Sampling of Particle-Associated Microcystins and BMAA Pilot Study in Lee County, Florida: Fall 2018–Winter 2019*; Florida Gulf Coast University: Fort Myers, FL, USA, 2019.
68. Desforges, J.P.; Mikkelsen, B.; Dam, M.; Riget, F.; Sveegaard, S.; Sonne, C.; Dietz, R.; Basu, N. Mercury and neurochemical biomarkers in multiple brain regions of five Arctic marine mammals. *Neurotoxicology* **2021**, *84*, 136–145. [[CrossRef](#)] [[PubMed](#)]
69. Joiris, C.R.; Holsbeek, L.; Bolbat, D.; Gascard, C.; Stanev, T.; Komakhidze, A.; Baumgartner, W.; Birkun, A. Total and organic mercury in the Black Sea harbour porpoise *Phocoena phocoena* relicta. *Mar. Pollut. Bull.* **2001**, *42*, 905–911. [[CrossRef](#)]
70. Van Elk, C.; van de Bildt, M.; van Run, P.; de Jong, A.; Getu, S.; Verjans, G.; Osterhaus, A.; Kuiken, T. Central nervous system disease and genital disease in harbor porpoises (*Phocoena phocoena*) are associated with different herpesviruses. *Vet. Res.* **2016**, *47*, 28. [[CrossRef](#)]
71. Rubio-Guerri, C.; Melero, M.; Esperon, F.; Belliere, E.N.; Arbelo, M.; Crespo, J.L.; Sierra, E.; Garcia-Parraga, D.; Sanchez-Vizcaino, J.M. Unusual striped dolphin mass mortality episode related to cetacean morbillivirus in the Spanish Mediterranean sea. *BMC Vet. Res.* **2013**, *9*, 106. [[CrossRef](#)]
72. Guzman-Verri, C.; Gonzalez-Barrientos, R.; Hernandez-Mora, G.; Morales, J.A.; Baquero-Calvo, E.; Chaves-Olarte, E.; Moreno, E. Brucella ceti and brucellosis in cetaceans. *Front. Cell Infect. Microbiol.* **2012**, *2*, 3. [[CrossRef](#)]
73. Leblanc, P.; Vorberg, I.M. Viruses in neurodegenerative diseases: More than just suspects in crimes. *PLoS Pathog.* **2022**, *18*, e1010670. [[CrossRef](#)]
74. Geraci, J.R.; Lounsbury, V.L.; Yates, N. *Marine Mammals Ashore, A Field Guide for Strandings*, 2nd ed.; National Aquarium in Baltimore, Inc.: Baltimore, MD, USA, 2005; pp. 198–199.
75. Breathnach, A.S.; Goldby, F. The amygdaloid nuclei, hippocampus and other parts of the rhinencephalon in the porpoise (*Phocoena phocoena*). *J. Anat.* **1954**, *88*, 267–291.
76. Marino, L.; Sudheimer, K.; Sarko, D.; Sirpenski, G.; Johnson, J.I. Neuroanatomy of the harbor porpoise (*Phocoena phocoena*) from magnetic resonance images. *J. Morphol.* **2003**, *257*, 308–347. [[CrossRef](#)] [[PubMed](#)]
77. LeDuc, R.G.; Perrin, W.F.; Dizon, A.E. Phylogenetic Relationships Among the Delphinid Cetaceans Based on Full Cytochrome B Sequences. *Mar. Mammal Sci.* **1999**, *15*, 619–648. [[CrossRef](#)]

78. Chen, I.H.; Chou, L.S.; Chou, S.J.; Wang, J.H.; Stott, J.; Blanchard, M.; Jen, I.F.; Yang, W.C. Selection of suitable reference genes for normalization of quantitative RT-PCR in peripheral blood samples of bottlenose dolphins (*Tursiops truncatus*). *Sci. Rep.* **2015**, *5*, 15425. [[CrossRef](#)]
79. Schmittgen, T.D.; Livak, K.J. Analyzing real-time PCR data by the comparative C(T) method. *Nat. Protoc.* **2008**, *3*, 1101–1108. [[CrossRef](#)]
80. Su, A.I.; Cooke, M.P.; Ching, K.A.; Hakak, Y.; Walker, J.R.; Wiltshire, T.; Orth, A.P.; Vega, R.G.; Sapinoso, L.M.; Moqrich, A.; et al. Large-scale analysis of the human and mouse transcriptomes. *Proc. Natl. Acad. Sci. USA* **2002**, *99*, 4465–4470. [[CrossRef](#)]
81. Mirra, S.S.; Hart, M.N.; Terry, R.D. Making the diagnosis of Alzheimer's disease. A primer for practicing pathologists. *Arch. Pathol. Lab. Med.* **1993**, *117*, 132–144. [[PubMed](#)]

Disclaimer/Publisher's Note: The statements, opinions and data contained in all publications are solely those of the individual author(s) and contributor(s) and not of MDPI and/or the editor(s). MDPI and/or the editor(s) disclaim responsibility for any injury to people or property resulting from any ideas, methods, instructions or products referred to in the content.